Cross-sectional evaluation of humoral responses against SARS-CoV-2 Spike

Jérémie Prévost[1,2,*], Romain Gasser[1,2,*], Guillaume Beaudoin-Bussières[1,2,*], Jonathan Richard[1,2*], Ralf Duerr[3*] Annemarie Laumaea[1,2,*], Sai Priya Anand[1,4], Guillaume Goyette[1], Shilei Ding[1,2], Halima Medjahed[1], Antoine Lewin[5], Josée Perreault[5], Tony Tremblay[5], Gabrielle Gendron-Lepage[1], Nicolas Gauthier[6], Marc Carrier[7], Diane Marcoux[8], Alain Piché[9], Myriam Lavoie[10], Alexandre Benoit[11], Vilayvong Loungnarath[12], Gino Brochu[13], Marc Desforges[14,15], Pierre J. Talbot[14], Graham T. Gould Maule[16], Marceline Côté[16], Christian Therrien[17], Bouchra Serhir[17], Renée Bazin[5], Michel Roger[1,2,17] and Andrés Finzi[1,2,4,#]

[1]Centre de Recherche du CHUM, QC H2X 0A9, Canada
[2]Département de Microbiologie, Infectiologie et Immunologie, Université de Montréal, Montreal, QC H2X 0A9, Canada
[3]Department of Pathology, New York University School of Medicine, New York, NY 10016, USA
[4]Department of Microbiology and Immunology, McGill University, Montreal, QC H3A 2B4, Canada
[5]Héma-Québec, Affaires Médicales et Innovation, Québec, QC, G1V 5C3, Canada
[6]Hôpital Sacré-Cœur de Montréal, Montreal, QC H4J 1C5, Canada
[7]Hôpital Cité-de-la-Santé, Laval, QC H7M 3L9, Canada
[8]Hôtel-Dieu de Lévis, Lévis, QC G6V 3Z1, Canada
[9]Centre Hospitalier Universitaire de Sherbrooke, Sherbrooke, QC J1H 5H4, Canada
[10]CIUSSS du Saguenay-Lac-Saint-Jean, Hôpital de Chicoutimi, Chicoutimi, QC G7H 5H6, Canada
[11]Hôpital de Verdun, Montreal, QC H4G 2A3, Canada
[12]CHU de Québec, Hôpital Enfant-Jésus, Quebec, QC G1J 1Z4, Canada
[13]CIUSSS de la Mauricie-et-du-Centre-du-Québec, Trois-Rivières, QC G9A 5C5, Canada
[14]INRS-Institut Armand Frappier, Laval, QC H7V 1B7, Canada
[15]CHU Ste-Justine, Montreal, QC, H3T 1C5, Canada
[16]Department of Biochemistry, Microbiology and Immunology, and Center for Infection, Immunity, and Inflammation, University of Ottawa, Ottawa, ON K1H 8M5, Canada
[17]Laboratoire de Santé Publique du Québec, Institut national de santé publique du Québec, Sainte-Anne-de-Bellevue H9X 3R5, Canada

*Contributed equally

[#] Correspondence: andres.finzi@umontreal.ca

Running Title: Antibody responses against SARS-CoV-2 S

Key Words: Coronavirus, COVID-19, SARS-CoV-2, Spike glycoproteins, RBD, ELISA, IgM, IgG, neutralization, cross-reactivity

Word Count for Summary: 168

Word Count for the Body of the Text: 1149

SUMMARY

The SARS-CoV-2 virus is responsible for the current worldwide coronavirus disease 2019 (COVID-19) pandemic, infecting millions of people and causing hundreds of thousands of deaths. The Spike glycoprotein of SARS-CoV-2 mediates viral entry and is the main target for neutralizing antibodies. Understanding the antibody response directed against SARS-CoV-2 is crucial for the development of vaccine, therapeutic and public health interventions. Here we performed a cross-sectional study on 98 SARS-CoV-2-infected individuals to evaluate humoral responses against the SARS-CoV-2 Spike. The vast majority of infected individuals elicited anti-Spike antibodies within 2 weeks after the onset of symptoms. The levels of receptor-binding domain (RBD)-specific IgG persisted overtime, while the levels of anti-RBD IgM decreased after symptoms resolution. Some of the elicited antibodies cross-reacted with other human coronaviruses in a genus-restrictive manner. While most of individuals developed neutralizing antibodies within the first two weeks of infection, the level of neutralizing activity was significantly decreased over time. Our results highlight the importance of studying the persistence of neutralizing activity upon natural SARS-CoV-2 infection.

64 **MAIN**

65 The first step in the replication cycle of coronaviruses (CoV) is viral entry. This is
66 mediated by their trimeric Spike (S) glycoproteins. Similar to SARS-CoV, the S glycoprotein of
67 SARS-CoV-2 interacts with angiotensin-converting enzyme 2 (ACE2) as its host receptor[1-3].
68 During entry, the Spike binds the host cell through interaction between its receptor binding
69 domain (RBD) and ACE2 and is cleaved by cell surface proteases or endosomal cathepsins[1,4,5],
70 triggering irreversible conformational changes in the S protein enabling membrane fusion and
71 viral entry[6,7]. The SARS-CoV-2 Spike is very immunogenic, with RBD representing the main
72 target for neutralizing antibodies[8-11]. Humoral responses are important for preventing and
73 controlling viral infections[12,13]. However, little is known about the chronology and durability of
74 the human antibody response against SARS-CoV-2.

75

76 Here we analyzed serological samples from 98 SARS-CoV-2-infected individuals at
77 different times post-infection and 10 uninfected individuals for their reactivity to SARS-CoV-2 S
78 glycoprotein, cross-reactivity with other human CoV (HCoV), as well as virus neutralization.
79 Samples were collected from COVID-19 positive individuals starting on March 2020 or healthy
80 individuals before the COVID-19 outbreak (COVID-19 negative). Cross-sectional serum
81 samples (n= 71) were collected from individuals presenting typical clinical symptoms of acute
82 SARS-CoV-2 infection (Extended Table 1). All patients were positive for SARS-CoV-2 by RT-
83 PCR on nasopharyngeal specimens. The average age of the infected patients was 56 years old,
84 including 31 males and 40 females. Samples were classified into 3 different time points after
85 infection: 24 (11 males, 13 females) were obtained at 2-7 days (T1, median = 3 days), 20 (9
86 males, 11 females) between 8-14 days (T2, median = 11 days) and 27 (11 males, 16 females)

87 between 16-30 days (T3, median = 23 days). Samples were also obtained from 27 convalescent
88 patients (20 males, 7 females, median = 42 days), who have been diagnosed with or tested
89 positive for COVID-19 with complete resolution of symptoms for at least 14 days.
90
91 We first evaluated the presence of RBD-specific IgG and IgM antibodies by ELISA[14,15].
92 The level of RBD-specific IgM peaked at T2 and was followed by a stepwise decrease over time
93 (T3 and Convalescent) (Figure 1). Three quarter of the patients had detectable anti-RBD IgM
94 two weeks after the onset of the symptoms. Similarly, 75% of patients in T2 developed anti-RBD
95 IgG, reaching 100% in convalescent patients. In contrast to IgM, the levels of RBD-specific IgG
96 peaked at T3 and remained relatively stable after complete resolution of symptoms (convalescent
97 patients).
98
99 We next used flow cytometry to examine the ability of sera to recognize the full-length
100 SARS-CoV-2 Spike expressed at the cell surface. Briefly, 293T cells expressing SARS-CoV-2 S
101 glycoproteins were stained with samples, followed by incubation with secondary antibodies
102 recognizing all antibody isotypes. As presented in Figure 2, 54.2% of the sera from T1 already
103 contained SARS-CoV-2 full Spike-reactive antibodies. Interestingly, the majority of patients
104 from T2, T3 and convalescent groups were found to be seropositive. Antibody levels targeting
105 the SARS-CoV-2 Spike significantly increased from T1 to T2/T3 and remained relatively stable
106 thereafter. As expected, the levels of antibodies recognizing the full Spike correlated with the
107 presence of both RBD-specific IgG and IgM (Extended Figure 1). We also evaluated potential
108 cross-reactivity against the closely related SARS-CoV Spike. None of the COVID-19 negative
109 samples recognized the SARS-CoV Spike. While the reactivity of COVID-19+ samples to

SARS-CoV S was lower than for SARS-CoV-2 S, it followed a similar progression and significantly correlated with their reactivity to SARS-CoV-2 full Spike or RBD protein (Figure 2 and Extended Figure 1). This indicates that SARS-CoV-2-elicited antibodies cross-react with human *Sarbecoviruses.* This was also observed with another *Betacoronavirus* (OC43) but not with *Alphacoronavirus* (NL63, 229E) S glycoproteins, suggesting a genus-restrictive cross-reactivity (Figure 2c and Extended Figure 1). This differential cross-reactivity could be explained by the high degree of conservation in the S protein, particularly in the S2 subunit among *Betacoronaviruses*[16-18].

We next measured the capacity of patient samples to neutralize pseudoparticles bearing SARS-CoV-2 S, SARS-CoV S or VSV-G glycoproteins using 293T cells stably expressing ACE2 as target cells (Figure 3 and Extended Figure 2). Neutralizing activity, as measured by the neutralization half-maximum inhibitory dilution (ID_{50}) or the neutralization 80% inhibitory dilution (ID_{80}), was detected in most patients within 2 weeks after the onset of symptoms (T2, T3 and Convalescent patients) (Figure 3). SARS-CoV-2 neutralization was specific since no neutralization was observed against pseudoparticles expressing VSV-G. The capacity to neutralize SARS-CoV-2 S-pseudotyped particles significantly correlated with the presence of RBD-specific IgG/IgM and anti-S antibodies (Extended Figure 3). While the percentage of patients eliciting neutralizing antibodies against SARS-CoV-2 Spike remained relatively stable 2 weeks after disease symptom onset (T2, T3 and Convalescent patients), neutralizing antibody titers significantly decreased after the complete resolution of symptoms as observed in the convalescent patients (Figure 3g,h). Cross-reactive neutralizing antibodies against SARS-CoV S protein (Figure 2b) were also detected in some SARS-CoV-2-infected individuals, but with

133 significantly lower potency and also waned over time. We note that around 40% of convalescent
134 patients did not exhibit any neutralizing activity. This suggests that the production of neutralizing
135 antibodies is not a prerequisite to the resolution of the infection and that other arms of the
136 immune system could be sufficient to control the infection in an important proportion of the
137 population.
138
139 This study helps to better understand the kinetics and persistence of humoral responses
140 directed against SARS-CoV-2 (Figure 4). Our results reveal that the vast majority of infected
141 individuals are able to elicit antibodies directed against SARS-CoV-2 Spike within 2 weeks after
142 symptom onset and persist after the resolution of the infection. Accordingly, all tested
143 convalescent patients were found to be seropositive. As expected, RBD-specific IgM levels
144 decreased over the duration of the study while IgG remained relatively stable. Our results
145 highlight how SARS-CoV-2 Spike, like other coronaviruses, appears to be relatively easily
146 recognized by Abs present in sera from infected individuals. This was suggested to be linked to
147 the higher processing of glycans compared to other type I fusion protein, such as HIV-1 Env,
148 Influenza A HA or filoviruses GP[19,20]. The ease of naturally-elicited Abs to recognize the Spike
149 might be associated with the low rate of somatic hypermutation observed in neutralizing Abs[9].
150 This low somatic hypermutation rate could in turn explain why the majority of the SARS-CoV-2
151 infected individuals are able to generate neutralizing antibodies within only two weeks after
152 infection (Figure 3). In contrast, the development of potent neutralizing antibodies against HIV-1
153 Env usually requires 2-3 years of infection and require a high degree of somatic hypermutation[21].
154 Nevertheless, in the case of SARS-CoV-2 infection, the neutralization capacity decreases
155 significantly 6 weeks after the onset of symptoms, following a similar trend as anti-RBD IgM

156 (Figure 4). Interestingly, anti-RBD IgM presented a stronger correlation with neutralization than
157 IgG (Extended Figure 3a), suggesting that at least part of the neutralizing activity is mediated by
158 IgM. However, it remains unclear whether this reduced level of neutralizing activity would
159 remain sufficient to protect from re-infection.
160
161

AUTHOR CONTRIBUTIONS

J.Prévost, J.R., B.S., R.B., M.R. and A.F. conceived the study. J.Prévost, J.R., A.F. designed experimental approaches; J.Prévost, G.B.B., R.G., A.Laumaea, J.R., S.P.A., G.G., S.D., T.T., J.Perreault, A.Lewin., R.D. R.B., M.R., and A.F. performed, analyzed and interpreted the experiments; J.Prévost, G.B.B., J.R., H.M., G.G.-L., M.D., P.T., G.T.G.M., M.Côté and A.F. contributed novel reagents; N.G., M.Carrier, D.M., A.P., M.L., A.B., V.L., G.B., C.T., R.B. and M.R. collected clinical samples; J.Prévost, J.R. and A.F. wrote the paper. Every author has read edited and approved the final manuscript.

ACKNOWLEDGMENTS

The authors thank the CRCHUM BSL3 and Flow Cytometry Platforms for technical assistance. We thank Dr Florian Krammer (Icahn School of Medicine at Mount Sinai, NY) for the plasmid expressing the SARS-CoV-2 RBD domain, Dr Stefan Pöhlmann (Georg-August University, Germany) for the plasmids coding for SARS-CoV S, SARS-CoV-2 S and hCoV 229E and NL63 S glycoproteins and Dr M. Gordon Joyce (U.S. MHRP) for the monoclonal antibody CR3022. We also thank Danka K Shank and Melina Bélanger Collard from the Laboratoire de Santé Publique du Québec for their help in preparing the specimens. This work was supported by le Ministère de l'Économie et de l'Innovation du Québec, Programme de soutien aux organismes de recherche et d'innovation to A.F and by the Fondation du CHUM. This work was also supported by a CIHR foundation grant #352417 to A.F. Development of SARS-CoV-2 reagents was partially supported by the NIAID Centers of Excellence for Influenza Research and Surveillance (CEIRS) contract HHSN272201400008C. A.F. is the recipient of a Canada Research Chair on Retroviral Entry # RCHS0235 950-232424. R.D. was supported by NIH grant

R01 AI122953-05. M.C. is the recipient of a Tier II Canada Research Chair in Molecular Virology and Antiviral Therapeutics and an Ontario's Early Researcher Award. J.P., G.B.B. and S.P.A are supported by CIHR fellowships. R.G. is supported by a MITACS Accélération postdoctoral fellowship. The funders had no role in study design, data collection and analysis, decision to publish, or preparation of the manuscript.

Competing interests

The authors declare no competing interests.

METHODS

Ethics statement

All work was conducted in accordance with the Declaration of Helsinki in terms of informed consent and approval by an appropriate institutional board. In addition, this study was conducted in accordance with the rules and regulations concerning ethical reviews in Quebec, particularly those specified in the Civil Code (http://legisquebec.gouv.qc.ca/fr/ShowDoc/cs/CCQ-1991) and in subsequent IRB practice. Informed Consent was obtained for all participating subjects and the study was approved by Quebec Public health authorities. Convalescent plasmas were obtained from donors who consented to participate in this research project (REB # 2020-004). The donors were recruited by Héma-Québec and met all donor eligibility criteria for routine apheresis plasma donation, plus two additional criteria: previous confirmed COVID-19 infection and complete resolution of symptoms for at least 14 days.

Plasmids

The plasmids expressing the human coronavirus Spikes of SARS-CoV-2, SARS-CoV, NL63 and 229E were previously reported[1,22]. The OC43 Spike with an N-terminal 3xFlag tag and C-terminal 17 residue deletion was cloned into pCAGGS following amplification of the spike gene from pB-Cyst-3FlagOC43SC17 (kind gift of James M. Rini, University of Toronto, ON, Canada). The plasmid encoding for SARS-CoV-2 S RBD (residues 319-541) fused with a hexahistidine tag was reported elsewhere[15]. The vesicular stomatitis virus G (VSV-G)-encoding plasmid (pSVCMV-IN-VSV-G) was previously described[23]. The lentiviral packaging plasmids pLP1 and pLP2, coding for HIV-1 *gag/pol* and *rev* respectively, were purchased from Invitrogen.

The transfer plasmid (pLenti-C-mGFP-P2A-Puro-ACE2) encoding for human angiotensin converting enzyme 2 (ACE2) fused with a mGFP C-terminal tag and a puromycin selection marker was purchased from OriGene. The lentiviral vector to produce pseudoparticles was pNL4.3 R-E- Luc.

Cell lines

293T human embryonic kidney cells (obtained from ATCC) were maintained at 37°C under 5% CO_2 in Dulbecco's modified Eagle's medium (DMEM) (Wisent) containing 5% fetal bovine serum (VWR) and 100 µg/ml of penicillin-streptomycin (Wisent). For the generation of 293T cells stably expressing human ACE2, transgenic lentivirus were produced in 293T using a third-generation lentiviral vector system. Briefly, 293T cells were co-transfected with two packaging plasmids (pLP1 and pLP2), an envelope plasmid (pSVCMV-IN-VSV-G) and a lentiviral transfer plasmid coding for human ACE2 (pLenti-C-mGFP-P2A-Puro-ACE2) (OriGene). Forty-eight hours post-transfection, supernatant containing lentiviral particles was used to infect more 293T cells in presence of 5µg/mL polybrene. Stably transduced cells were enriched upon puromycin selection. 293T-ACE2 cells were then cultured in a medium supplemented with 2 µg/ml of puromycin (Sigma).

Sera and antibodies

Sera from SARS-CoV-2-infected and uninfected donors were collected, heat-inactivated for 1 hour at 56 °C and stored at -80°C until ready to use in subsequent experiments. The monoclonal antibody CR3022 was used to as a positive control in ELISA assays and was previously described [8,24,25]. Horseradish peroxidase (HRP)-conjugated antibody specific for the Fc region of

human IgG (Invitrogen) or for the Fc region of human IgM (Invitrogen) were used as secondary antibodies to detect sera binding in ELISA experiments. Alexa Fluor-647-conjugated goat anti-human IgG (H+L) Abs (Invitrogen) were used as secondary antibodies to detect sera binding in flow cytometry experiment. Polyclonal goat anti-ACE2 (RND systems) and Alexa-Fluor-conjugated donkey anti-goat IgG Abs (Invitrogen) were used to detect cell-surface expression of human ACE2.

Protein expression and purification

FreeStyle 293F cells (Invitrogen) were grown in FreeStyle 293F medium (Invitrogen) to a density of 1 x 10^6 cells/mL at 37°C with 8 % CO_2 with regular agitation (150 rpm). Cells were transfected with a plasmid coding for SARS-CoV-2 S RBD using ExpiFectamine 293 transfection reagent, as directed by the manufacturer (Invitrogen). One week later, cells were pelleted and discarded. Supernatants were filtered using a 0.22 µm filter (Thermo Fisher Scientific). The recombinant RBD proteins were purified by nickel affinity columns, as directed by the manufacturer (Invitrogen). The RBD preparations were dialyzed against phosphate-buffered saline (PBS) and stored in aliquots at -80°C until further use. To assess purity, recombinant proteins were loaded on SDS-PAGE gels and stained with Coomassie Blue. For cell-surface staining, RBD proteins were fluorescently labelled with Alexa Fluor 594 (Invitrogen) according to the manufacturer's protocol.

ELISA assay

Recombinant SARS-CoV-2 S RBD proteins (2.5 µg/ml), or bovine serum albumin (BSA) (2.5 µg/ml) as a negative control, were prepared in PBS and were adsorbed to plates (MaxiSorp;

Nunc) overnight at 4°C. Coated wells were subsequently blocked with blocking buffer (Tris-buffered saline [TBS] containing 0.1% Tween 20 and 2% [wt/vol] BSA) for 1 h at room temperature. Wells were then washed four times with washing buffer (Tris-buffered saline [TBS] containing 0.1% Tween 20). Anti-SARS-CoV-2 RBD CR3022 mAb (50 ng/ml) or sera from SARS-CoV-2-infected or uninfected donors (1:100, 1:250, 1:500, 1:1000, 1:2000, 1:4000 dilution) were diluted in blocking buffer and incubated with the RBD-coated wells for 1 h at room temperature. Plates were washed four times with washing buffer followed by incubation with secondary Abs (diluted in blocking buffer) for 1 h at room temperature, followed by four washes. HRP enzyme activity was determined after the addition of a 1:1 mix of Western Lightning oxidizing and luminol reagents (Perkin Elmer Life Sciences). Light emission was measured with a LB 941 TriStar luminometer (Berthold Technologies). Signal obtained with BSA was subtracted for each serum and were then normalized to the signal obtained with CR3022 mAb present in each plate. The seropositivity threshold was established using the following formula: mean RLU of all COVID-19 negative sera normalized to CR3022 + (3 standard deviations of the mean of all COVID-19 negative sera).

Flow cytometry analysis of cell-surface staining

Using the standard calcium phosphate method, 10 µg of Spike expressor and 2 µg of a green fluorescent protein (GFP) expressor (pIRES-GFP) was transfected into 2×10^6 293T cells. At 48h post transfection, 293T cells were stained with sera from SARS-CoV-2-infected or uninfected individuals (1:250 dilution). The percentage of transfected cells (GFP+ cells) was determined by gating the living cell population based on the basis of viability dye staining (Aqua Vivid, Invitrogen). Samples were acquired on a LSRII cytometer (BD Biosciences, Mississauga,

ON, Canada) and data analysis was performed using FlowJo vX.0.7 (Tree Star, Ashland, OR, USA). The seropositivity threshold was established using the following formula: (mean of all COVID-19 negative sera + (3 standard deviation of the mean of all COVID-19 negative sera) + inter-assay coefficient of variability).

Virus neutralization assay

Target cells were infected with single-round luciferase-expressing lentiviral particles. Briefly, 293T cells were transfected by the calcium phosphate method with the lentiviral vector pNL4.3 R-E- Luc (NIH AIDS Reagent Program) and a plasmid encoding for SARS-CoV-2 Spike, SARS-CoV Spike or VSV-G at a ratio of 5:4. Two days after transfection, cell supernatants were harvested and stored in aliquots at –80°C until use. 293T-ACE2 target cells were seeded at a density of 1×10^4 cells/well in 96-well luminometer-compatible tissue culture plates (Perkin Elmer) 24 h before infection. Luciferase-expressing recombinant viruses in a final volume of 100 µl were incubated with the indicated sera dilutions (1/50; 1/250; 1/1250; 1/6250; 1/31250) for 1h at 37°C and were then added to the target cells followed by incubation for 48 h at 37°C; the medium was then removed from each well, and the cells were lysed by the addition of 30 µl of passive lysis buffer (Promega) followed by one freeze-thaw cycle. An LB 941 TriStar luminometer (Berthold Technologies) was used to measure the luciferase activity of each well after the addition of 100 µl of luciferin buffer (15 mM MgSO4, 15 mM KPO4 [pH 7.8], 1 mM ATP, and 1 mM dithiothreitol) and 50 µl of 1 mM d-luciferin potassium salt (Prolume). The neutralization half-maximal inhibitory dilution (ID_{50}) or the neutralization 80% inhibitory dilution (ID_{80}) represents the sera dilution to inhibit 50% or 80% of the infection of 293T-ACE2 cells by recombinant lentiviral viruses bearing the indicated surface glycoproteins.

Time series visualization

Area graphs were generated using RawGraphs with DensityDesign interpolation and the implemented normalization using vertically un-centered values[26].

Statistical analyses

Statistics were analyzed using GraphPad Prism version 8.0.2 (GraphPad, San Diego, CA, (USA). Every data set was tested for statistical normality and this information was used to apply the appropriate (parametric or nonparametric) statistical test. P values <0.05 were considered significant; significance values are indicated as * $p<0.05$, ** $p<0.01$, *** $p<0.001$, **** $p<0.0001$.

REFERENCES

1. Hoffmann, M., *et al.* SARS-CoV-2 Cell Entry Depends on ACE2 and TMPRSS2 and Is Blocked by a Clinically Proven Protease Inhibitor. *Cell* **181**, 271-280 e278 (2020).
2. Walls, A.C., *et al.* Unexpected Receptor Functional Mimicry Elucidates Activation of Coronavirus Fusion. *Cell* **176**, 1026-1039 e1015 (2019).
3. Shang, J., *et al.* Structural basis of receptor recognition by SARS-CoV-2. *Nature* (2020).
4. Ou, X., *et al.* Characterization of spike glycoprotein of SARS-CoV-2 on virus entry and its immune cross-reactivity with SARS-CoV. *Nat Commun* **11**, 1620 (2020).
5. Zang, R., *et al.* TMPRSS2 and TMPRSS4 promote SARS-CoV-2 infection of human small intestinal enterocytes. *Sci Immunol* **5**(2020).
6. Wrapp, D., *et al.* Cryo-EM structure of the 2019-nCoV spike in the prefusion conformation. *Science* **367**, 1260-1263 (2020).
7. Walls, A.C., *et al.* Structure, Function, and Antigenicity of the SARS-CoV-2 Spike Glycoprotein. *Cell* **181**, 281-292 e286 (2020).
8. Yuan, M., *et al.* A highly conserved cryptic epitope in the receptor binding domains of SARS-CoV-2 and SARS-CoV. *Science* **368**, 630-633 (2020).
9. Ju, B., *et al.* Human neutralizing antibodies elicited by SARS-CoV-2 infection. *Nature* (2020).
10. Shi, R., *et al.* A human neutralizing antibody targets the receptor binding site of SARS-CoV-2. *Nature* (2020).
11. Wu, Y., *et al.* A noncompeting pair of human neutralizing antibodies block COVID-19 virus binding to its receptor ACE2. *Science* (2020).

12. Murin, C.D., Wilson, I.A. & Ward, A.B. Antibody responses to viral infections: a structural perspective across three different enveloped viruses. *Nat Microbiol* **4**, 734-747 (2019).

13. Rouse, B.T. & Sehrawat, S. Immunity and immunopathology to viruses: what decides the outcome? *Nat Rev Immunol* **10**, 514-526 (2010).

14. Stadlbauer, D.*, et al.* SARS-CoV-2 Seroconversion in Humans: A Detailed Protocol for a Serological Assay, Antigen Production, and Test Setup. *Curr Protoc Microbiol* **57**, e100 (2020).

15. Amanat, F.*, et al.* A serological assay to detect SARS-CoV-2 seroconversion in humans. *Nat Med* (2020).

16. Jaimes, J.A., Andre, N.M., Chappie, J.S., Millet, J.K. & Whittaker, G.R. Phylogenetic Analysis and Structural Modeling of SARS-CoV-2 Spike Protein Reveals an Evolutionary Distinct and Proteolytically Sensitive Activation Loop. *J Mol Biol* **432**, 3309-3325 (2020).

17. Zhou, H.*, et al.* A Novel Bat Coronavirus Closely Related to SARS-CoV-2 Contains Natural Insertions at the S1/S2 Cleavage Site of the Spike Protein. *Curr Biol* (2020).

18. Madu, I.G., Roth, S.L., Belouzard, S. & Whittaker, G.R. Characterization of a highly conserved domain within the severe acute respiratory syndrome coronavirus spike protein S2 domain with characteristics of a viral fusion peptide. *J Virol* **83**, 7411-7421 (2009).

19. Watanabe, Y., Allen, J.D., Wrapp, D., McLellan, J.S. & Crispin, M. Site-specific glycan analysis of the SARS-CoV-2 spike. *Science* (2020).

20. Watanabe, Y.*, et al.* Vulnerabilities in coronavirus glycan shields despite extensive glycosylation. *Nat Commun* **11**, 2688 (2020).

21. Sok, D. & Burton, D.R. Recent progress in broadly neutralizing antibodies to HIV. *Nat Immunol* **19**, 1179-1188 (2018).

22. Hofmann, H.*, et al.* Human coronavirus NL63 employs the severe acute respiratory syndrome coronavirus receptor for cellular entry. *Proc Natl Acad Sci U S A* **102**, 7988-7993 (2005).

23. Lodge, R., Lalonde, J.P., Lemay, G. & Cohen, E.A. The membrane-proximal intracytoplasmic tyrosine residue of HIV-1 envelope glycoprotein is critical for basolateral targeting of viral budding in MDCK cells. *EMBO J* **16**, 695-705 (1997).

24. ter Meulen, J.*, et al.* Human monoclonal antibody combination against SARS coronavirus: synergy and coverage of escape mutants. *PLoS Med* **3**, e237 (2006).

25. Tian, X.*, et al.* Potent binding of 2019 novel coronavirus spike protein by a SARS coronavirus-specific human monoclonal antibody. *Emerg Microbes Infect* **9**, 382-385 (2020).

26. Mauri, M., Elli, T., Caviglia, G., Uboldi, G. & Azzi, M. RAWGraphs: A Visualisation Platform to Create Open Outputs. in *Proceedings of the 12th Biannual Conference on Italian SIGCHI Chapter* 5 (ACM, New York, NY, 2017).

Figure Legends

Figure 1. Detection of SARS-CoV-2 RBD-specific IgM and IgG over time.

Indirect ELISA was performed using recombinant SARS-CoV-2 RBD and incubated with samples from COVID-19 negative or COVID-19 positive patients at different times after symptoms onset (T1, T2, T3, Convalescent). Anti-RBD binding was detected using (a-c) anti-IgM-HRP or (d-f) anti-IgG-HRP. Relative light units (RLU) obtained with BSA (negative control) were subtracted and further normalized to the signal obtained with the anti-RBD CR3022 mAb present in each plate. Data in graphs represent RLU done in quadruplicate, with error bars indicating means ± SEM. Undetectable measures are represented as white symbols and limits of detection are plotted. (c,f) Areas under the curve (AUC) were calculated based on RLU datasets shown in (a,d) using GraphPad Prism software. Statistical significance was tested using Kruskal-Wallis tests with a Dunn's post-test (* $p < 0.05$; ** $p < 0.01$; *** $p < 0.001$; **** $p < 0.0001$).

Figure 2. SARS-CoV-2 infection elicits cross-reactive antibodies against other human *Betacoronaviruses*.

Cell-surface staining of 293T cells expressing full-length Spike (S) from different HCoV (a) SARS-CoV-2, (b) SARS-CoV, (c) OC43,NL63 and 229E with samples from COVID-19 negative or COVID-19 positive patients at different stage of infection (T1, T2, T3, Convalescent). The graphs shown represent the median fluorescence intensities (MFI). Undetectable measures are represented as white symbols and limits of detection are plotted.

Error bars indicate means ± SEM. Statistical significance was tested using Kruskal-Wallis tests with a Dunn's post-test (* $p < 0.05$; ** $p < 0.01$; *** $p < 0.001$; **** $p < 0.0001$).

Figure 3. Anti-Spike neutralizing antibody titers decrease over time.

Pseudoviral particles coding for the luciferase reporter gene and bearing the following glycoproteins: (a,d,g,h) SARS-CoV-2 S, (b,e,i) SARS-CoV S or (c,f) VSV-G were used to infect 293T-ACE2 cells. Pseudoviruses were incubated with serial dilutions of samples from COVID-19 negative or COVID-19 positive patients (T1, T2, T3, Convalescent) at 37°C for 1 h prior to infection of 293T-ACE2 cells. Infectivity at each dilution was assessed in duplicate and is shown as the percentage of infection without sera for each glycoproteins. (g,i) Neutralization half maximal inhibitory serum dilution (ID_{50}) and (h) ID_{80} values were determined using a normalized non-linear regression using Graphpad Prism software. Undetectable measures are represented as white symbols. Neutralizer represent patients with (g,i) an ID_{50} over 100 or (h) an ID_{80} .Statistical significance was tested using Mann-Whitney U tests (* $p < 0.05$; ** $p < 0.01$).

Figure 4. Kinetics of humoral responses at different stages of SARS-CoV-2 infection

Area plot showing time series of indicated immunological parameters for three time points (T1-T3) during acute infection and the convalescent stage. Average values are displayed that are normalized per parameter, as implemented in RawGraphs.

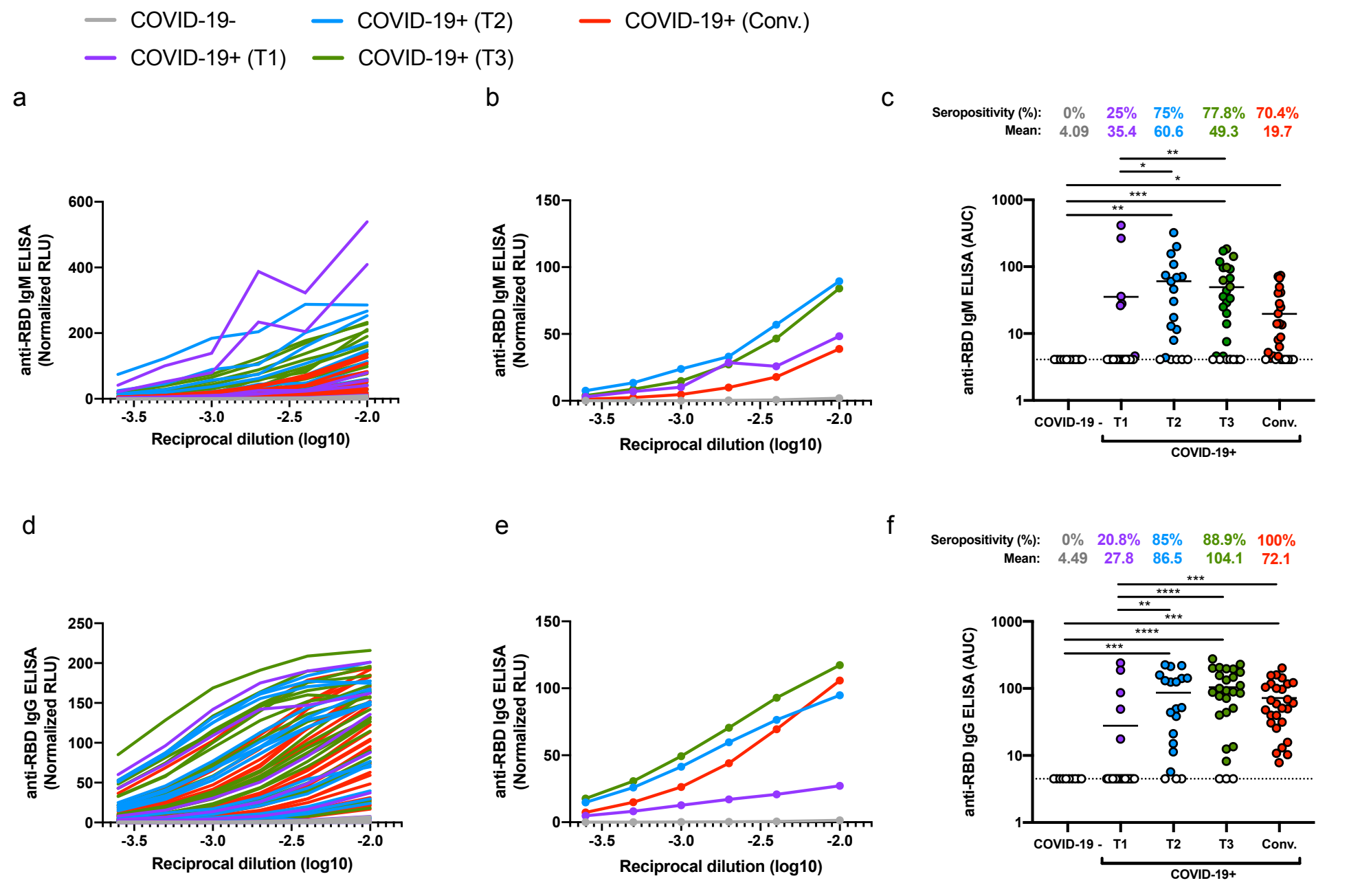
COVID-19-
COVID-19+ (T1)
COVID-19+ (T2)
COVID-19+ (T3)
COVID-19+ (Conv.)
a
anti-RBD IgM ELISA (Normalized RLU)
Reciprocal dilution (log10)
b
anti-RBD IgM ELISA (Normalized RLU)
Reciprocal dilution (log10)
c
Seropositivity (%): 0% 25% 75% 77.8% 70.4%
Mean: 4.09 35.4 60.6 49.3 19.7
anti-RBD IgM ELISA (AUC)
COVID-19 -
T1
T2
T3
Conv.
COVID-19+
d
anti-RBD IgG ELISA (Normalized RLU)
Reciprocal dilution (log10)
e
anti-RBD IgG ELISA (Normalized RLU)
Reciprocal dilution (log10)
f
Seropositivity (%): 0% 20.8% 85% 88.9% 100%
Mean: 4.49 27.8 86.5 104.1 72.1
anti-RBD IgG ELISA (AUC)
COVID-19 -
T1
T2
T3
Conv.
COVID-19+

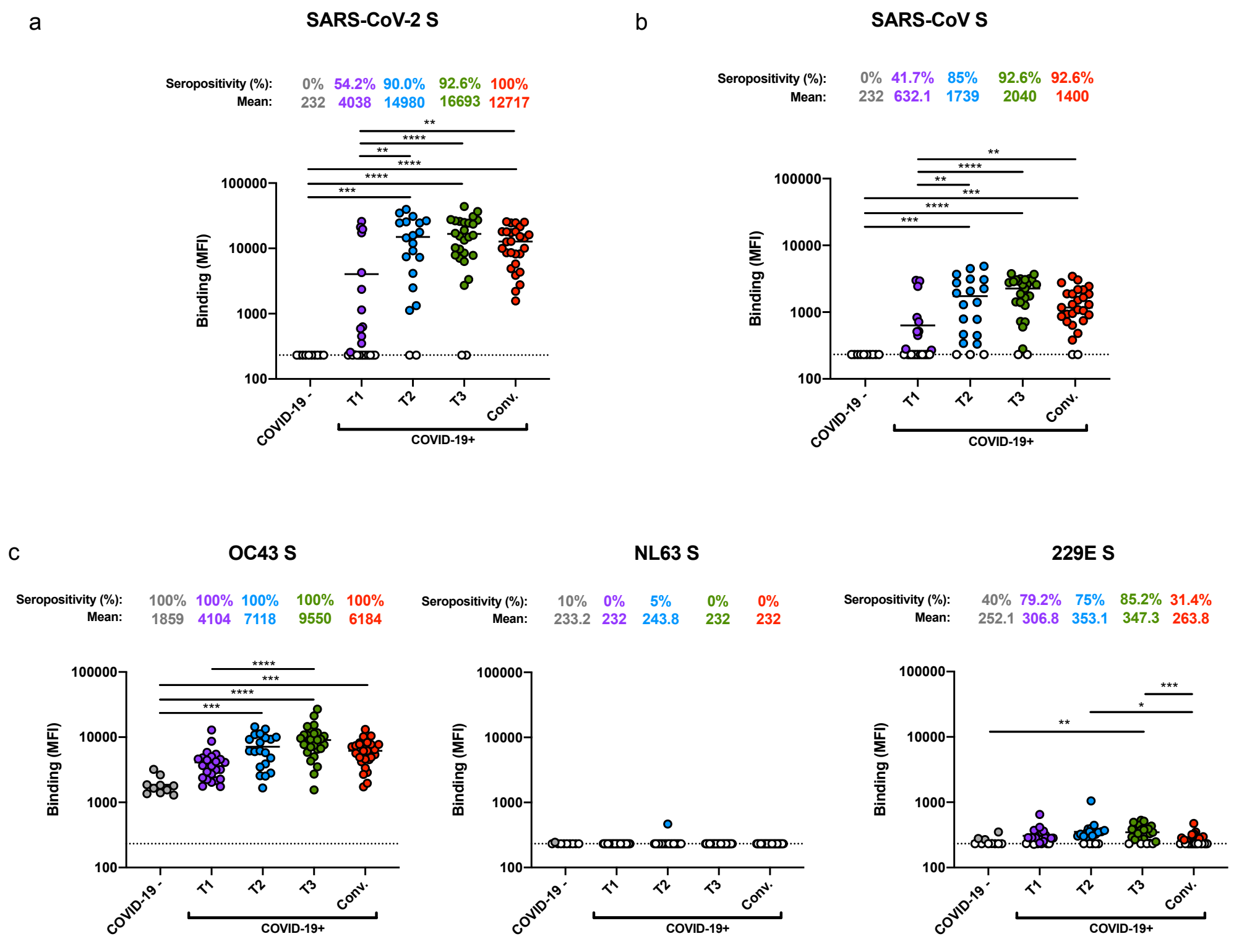
a
SARS-CoV-2 S
Seropositivity (%): 0% 54.2% 90.0% 92.6% 100%
Mean: 232 4038 14980 16693 12717
Binding (MFI)
100000
10000
1000
100
COVID-19 -
T1
T2
T3
Conv.
COVID-19+
b
SARS-CoV S
Seropositivity (%): 0% 41.7% 85% 92.6% 92.6%
Mean: 232 632.1 1739 2040 1400
c
OC43 S
Seropositivity (%): 100% 100% 100% 100% 100%
Mean: 1859 4104 7118 9550 6184
NL63 S
Seropositivity (%): 10% 0% 5% 0% 0%
Mean: 233.2 232 243.8 232 232
229E S
Seropositivity (%): 40% 79.2% 75% 85.2% 31.4%
Mean: 252.1 306.8 353.1 347.3 263.8

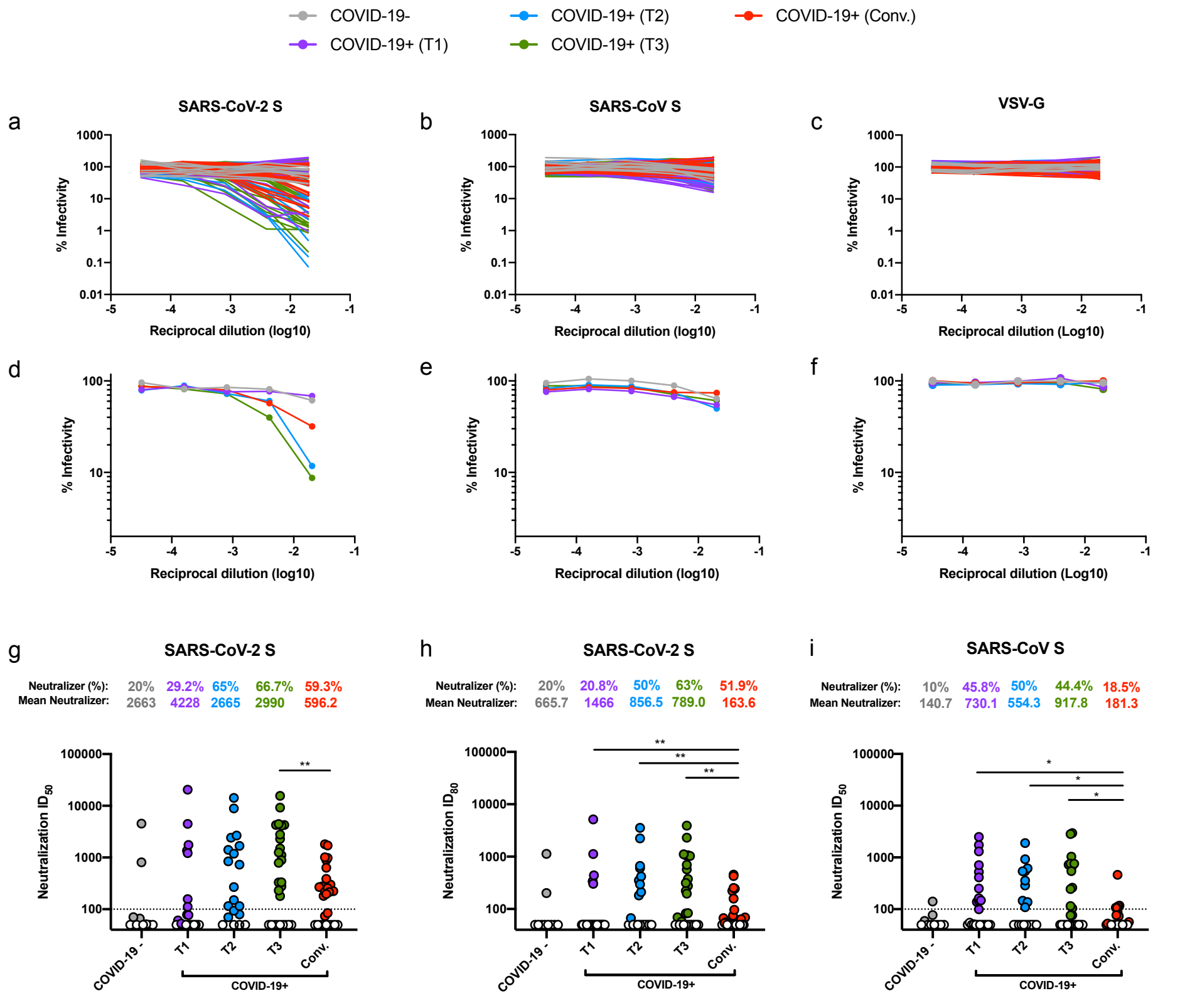
COVID-19-
COVID-19+ (T1)
COVID-19+ (T2)
COVID-19+ (T3)
COVID-19+ (Conv.)
a
SARS-CoV-2 S
% Infectivity
Reciprocal dilution (log10)
b
SARS-CoV S
c
VSV-G
Reciprocal dilution (Log10)
d
e
f
g
SARS-CoV-2 S
Neutralizer (%): 20% 29.2% 65% 66.7% 59.3%
Mean Neutralizer: 2663 4228 2665 2990 596.2
Neutralization ID50
COVID-19 -
T1
T2
T3
Conv.
COVID-19+
h
SARS-CoV-2 S
Neutralizer (%): 20% 20.8% 50% 63% 51.9%
Mean Neutralizer: 665.7 1466 856.5 789.0 163.6
Neutralization ID80
i
SARS-CoV S
Neutralizer (%): 10% 45.8% 50% 44.4% 18.5%
Mean Neutralizer: 140.7 730.1 554.3 917.8 181.3

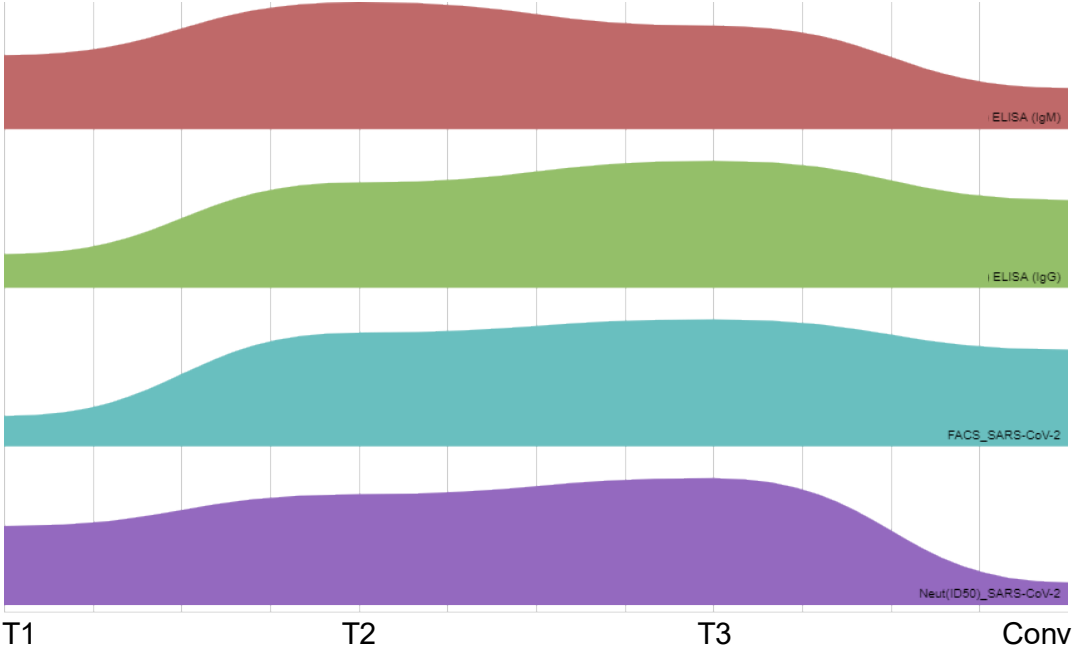
ELISA (IgM)
ELISA (IgG)
FACS_SARS-CoV-2
Neut(ID50)_SARS-CoV-2
T1
T2
T3
Conv

Supplemental Information

Supplemental information includes 2 tables and 3 figures, and can be found online.

Extended Table 1. Cross-sectional SARS-CoV-2 cohort clinical characteristics

Extended Table 2. Serological analysis of samples from SARS-CoV-2 infected individuals

Extended Figure 1. Detection of antibodies against cell-surface expressed SARS-CoV-2 full Spike correlates with RBD-specific IgG and IgM.

(a,c,e,g,i) Levels of recognition of the different human coronavirus Spikes (SARS-CoV-2 S, SARS-CoV, OC43 S, NL63 S, 229E S) evaluated by flow cytometry (Figure 2) were plotted against the levels of anti-RBD IgG and IgM evaluated by indirect ELISA (Figure 1). (b,d,f,h) Levels of recognition of different HCoV Spikes (SARS-CoV, OC43 S, NL63 S, 229E S) evaluated by flow cytometry were plotted against the levels of recognition of SARS-CoV-2 S (also evaluated by flow cytometry). Statistical analysis was performed using Spearman rank correlation tests.

Extended Figure 2. Characterization of 293T-ACE2 cell line

Cell-surface staining of 293T cells and 293T stably expressing human ACE2 (293T-ACE2) with (a) polyclonal goat anti-ACE2 or (b) RBD conjugated with Alexa Fluor 594 (RBD-AF594). Shown in (a,b) are histograms depicting representative anti-ACE2 and RBD-AF594 staining. (c) Recombinant pseudovirus expressing luciferase and bearing SARS-CoV-2 or VSV-G glycoproteins were used to infect 293T or 293T-ACE2 and infectivity was quantified by luciferase activity in cell lysate by relative light units (RLU).

Extended Figure 3. Anti-RBD antibodies positively correlate with neutralization.

(a) The neutralization ID_{50} with SARS-CoV-2 S was correlated with the levels of anti-RBD IgG and IgM quantified by ELISA or (b) with the level of anti-SARS-CoV-2 S antibodies quantified by flow cytometry. Statistical significance was tested using Spearman rank correlation tests.

Extended Data Table 1. Cross-sectional SARS-CoV-2 cohort

Group	n	Time (median)	Age (average)	Gender	
				Male (n)	Female (n)
T1	24	3 (2-7)	55 (31-94)	11	13
T2	20	11 (8-14)	63 (34-90)	9	11
T3	27	23 (16-30)	51 (20-93)	11	16
Convalescent	27	42 (23-52)	42 (19-69)	20	7

Extended Data Table 2. Serological analysis of samples from SARS-CoV-2 infected individuals

		FACS (MFI)					ELISA anti-RBD (AUC)		Neutralization (ID50)	
Patient ID	Group	SARS-CoV S	SARS-CoV-2 S	OC43 S	NL63 S	229E S	IgG	IgM	SARS-CoV S	SARS-CoV-2 S
1	T1	232	451	3664	232	313	4,49	4,09	250,63	156,47
2	T1	232	232	1743	232	232	4,49	4,09	0,00	0,00
3	T1	2990	25903	12877	232	284	239,90	266,10	1739,43	4476,28
4	T1	831	4270	4831	232	356	17,60	35,98	0,00	78,31
5	T1	448	631	5852	232	372	4,49	4,61	524,38	1353,00
6	T1	2924	21146	4629	232	227	86,39	415,00	0,00	1211,53
7	T1	232	350	5471	232	311	4,49	4,09	54,67	0,00
8	T1	232	232	3190	232	232	4,49	4,09	0,00	0,00
9	T1	232	232	2152	232	344	4,49	4,09	51,20	60,53
10	T1	232	232	4100	232	285	4,49	4,09	0,00	0,00
11	T1	2435	17303	8659	232	651	49,05	28,00	1304,97	1752,85
12	T1	232	232	3155	232	372	4,49	4,09	0,00	0,00
13	T1	232	232	5030	232	285	4,49	4,09	709,22	76,80
14	T1	270	590	4557	232	362	4,49	4,09	99,60	0,00
15	T1	718	19719	2707	232	232	187,80	26,14	137,97	20533,88
16	T1	232	232	2945	232	287	4,49	4,09	0,00	0,00
17	T1	232	1140	1762	232	233	4,49	4,09	0,00	0,00
18	T1	232	232	4452	232	232	4,49	4,09	0,00	0,00
19	T1	517	234	3598	232	283	4,49	4,09	145,33	0,00
20	T1	232	232	2270	232	287	4,49	4,09	162,42	52,85
21	T1	510	2356	2031	232	281	4,49	4,09	2497,50	111,87
22	T1	232	232	2237	232	413	4,49	4,09	147,54	0,00
23	T1	280	257	4206	232	251	4,49	4,09	411,52	0,00
24	T1	232	232	2380	232	238	4,49	4,09	0,00	0,00
25	T2	1399	14478	9308	232	232	49,65	17,40	0,00	115,05
26	T2	4493	39640	14425	232	354	219,10	199,40	540,54	1402,52
27	T2	332	1325	2810	232	232	5,70	4,09	0,00	0,00
28	T2	341	11926	1664	232	321	124,80	155,90	145,48	2412,55
29	T2	782	9188	6132	232	232	51,97	7,96	0,00	0,00
30	T2	447	7454	4791	232	342	21,14	11,48	0,00	69,88
31	T2	2743	34747	8276	232	303	213,50	46,18	0,00	727,27
32	T2	3144	25468	9244	232	293	140,80	322,70	287,27	2662,41
33	T2	232	232	3888	232	391	4,49	4,09	0,00	0,00
34	T2	2067	24488	9993	232	232	158,70	108,50	137,12	8904,72
35	T2	790	1122	2563	467	1048	4,49	4,09	0,00	0,00
36	T2	3686	17679	10901	232	232	142,40	60,33	921,66	267,67
37	T2	1927	26403	6020	232	326	224,40	71,17	1890,72	14178,36
38	T2	232	2495	3489	232	302	15,06	4,09	0,00	79,30
39	T2	464	4142	6185	232	399	11,33	4,38	614,63	149,99
40	T2	2243	15808	9780	232	346	130,50	68,94	108,89	843,17
41	T2	1293	7294	5772	232	355	38,45	12,87	356,13	1675,60
42	T2	4868	30938	13324	232	370	43,95	74,30	0,00	1184,97
43	T2	232	232	2532	232	307	4,49	4,09	540,83	93,37
44	T2	3073	24535	11264	232	445	124,90	30,34	0,00	115,31
45	T3	3175	15418	10990	232	395	92,55	92,04	1037,56	1105,22
46	T3	3016	25909	8125	232	386	201,50	96,50	260,42	1499,25
47	T3	2634	24951	10356	232	332	228,90	43,84	0,00	276,85
48	T3	3686	26501	13482	232	391	195,10	67,27	104,66	887,31
49	T3	1428	3351	6496	232	529	50,75	4,58	2954,21	179,82
50	T3	723	8490	4998	232	232	76,63	4,62	0,00	0,00
51	T3	1396	7833	9176	232	330	43,99	35,77	2834,47	9208,10
52	T3	1263	7064	5836	232	274	40,10	4,09	0,00	0,00
53	T3	2583	13350	10850	232	446	87,89	14,00	244,68	788,02
54	T3	3161	19011	15261	232	386	88,59	20,06	0,00	0,00
55	T3	2264	27040	11678	232	514	156,50	29,01	76,51	2288,33
56	T3	232	232	3511	232	280	4,49	4,09	0,00	0,00
57	T3	1747	14934	21177	232	232	100,70	33,47	0,00	329,92
58	T3	1641	9732	7461	232	391	8,22	4,09	0,00	0,00
59	T3	2575	43788	26862	232	433	205,40	118,80	0,00	4255,32
60	T3	281	2714	4297	232	293	12,51	4,12	722,02	229,94
61	T3	232	232	1553	232	236	4,49	4,09	75,99	0,00
62	T3	2919	17013	9604	232	374	13,49	4,09	0,00	0,00
63	T3	1878	15855	7696	232	268	71,25	50,23	0,00	332,23
64	T3	711	10219	14607	232	494	133,50	142,70	0,00	1252,98
65	T3	3053	30735	7638	232	346	196,80	184,50	114,73	4258,94
66	T3	3770	24356	9342	232	390	85,23	24,97	681,20	4123,71
67	T3	3067	36647	11330	232	232	147,00	172,40	759,88	2782,42
68	T3	2774	23502	6692	232	333	175,20	97,95	755,29	15586,03
69	T3	2861	27590	9046	232	232	275,80	62,70	544,37	4444,44
70	T3	599	6316	2720	232	378	4,49	4,09	0,00	0,00
71	T3	1412	7916	7058	232	249	110,50	7,55	0,00	73,21
72	Convalescent	2179	18055	7778	232	257	143,90	67,60	0,00	887,31
73	Convalescent	232	2775	2685	232	232	15,69	8,86	73,10	631,31
74	Convalescent	742	8550	4515	232	232	30,54	6,33	0,00	181,00
75	Convalescent	1172	10054	8280	232	265	60,59	13,99	462,11	979,43
76	Convalescent	232	2205	6135	232	320	10,82	4,09	76,57	298,42
77	Convalescent	3044	25170	7781	232	278	59,04	71,09	0,00	276,40
78	Convalescent	1655	15237	4901	232	232	39,86	4,09	0,00	0,00
79	Convalescent	911	8625	4588	232	474	68,48	5,22	0,00	267,95
80	Convalescent	1056	16116	4911	232	312	117,20	28,04	106,91	1806,68
81	Convalescent	864	8202	7062	232	232	39,63	4,60	0,00	0,00
82	Convalescent	381	1569	1968	232	232	13,02	4,09	0,00	0,00
83	Convalescent	3431	24732	8195	232	232	104,30	41,20	117,27	217,72
84	Convalescent	1862	17395	7403	232	232	116,70	73,81	0,00	223,36
85	Convalescent	1509	12831	5386	232	232	121,60	24,84	88,57	1706,19
86	Convalescent	958	5784	6278	232	232	49,68	4,09	0,00	0,00
87	Convalescent	2434	17985	10192	232	284	50,63	40,18	0,00	254,91
88	Convalescent	2171	21444	13151	232	232	159,80	19,93	0,00	0,00
89	Convalescent	1086	25681	6177	232	296	201,80	13,49	0,00	0,00
90	Convalescent	2751	18042	10467	232	327	155,70	49,73	0,00	1011,94
91	Convalescent	1877	24491	7723	232	232	97,20	4,09	0,00	214,50
92	Convalescent	720	9995	3355	232	351	66,59	14,12	114,35	73,75
93	Convalescent	1299	12623	7128	232	232	25,44	8,07	0,00	0,00
94	Convalescent	1309	8246	5663	232	232	31,52	4,25	0,00	0,00
95	Convalescent	637	4335	2877	232	232	7,81	4,09	106,09	385,36
96	Convalescent	930	4893	6456	232	232	47,88	4,09	0,00	0,00
97	Convalescent	481	3878	1729	232	247	10,29	4,57	52,77	196,23
98	Convalescent	1883	14455	4195	232	232	100,70	4,09	56,40	84,53

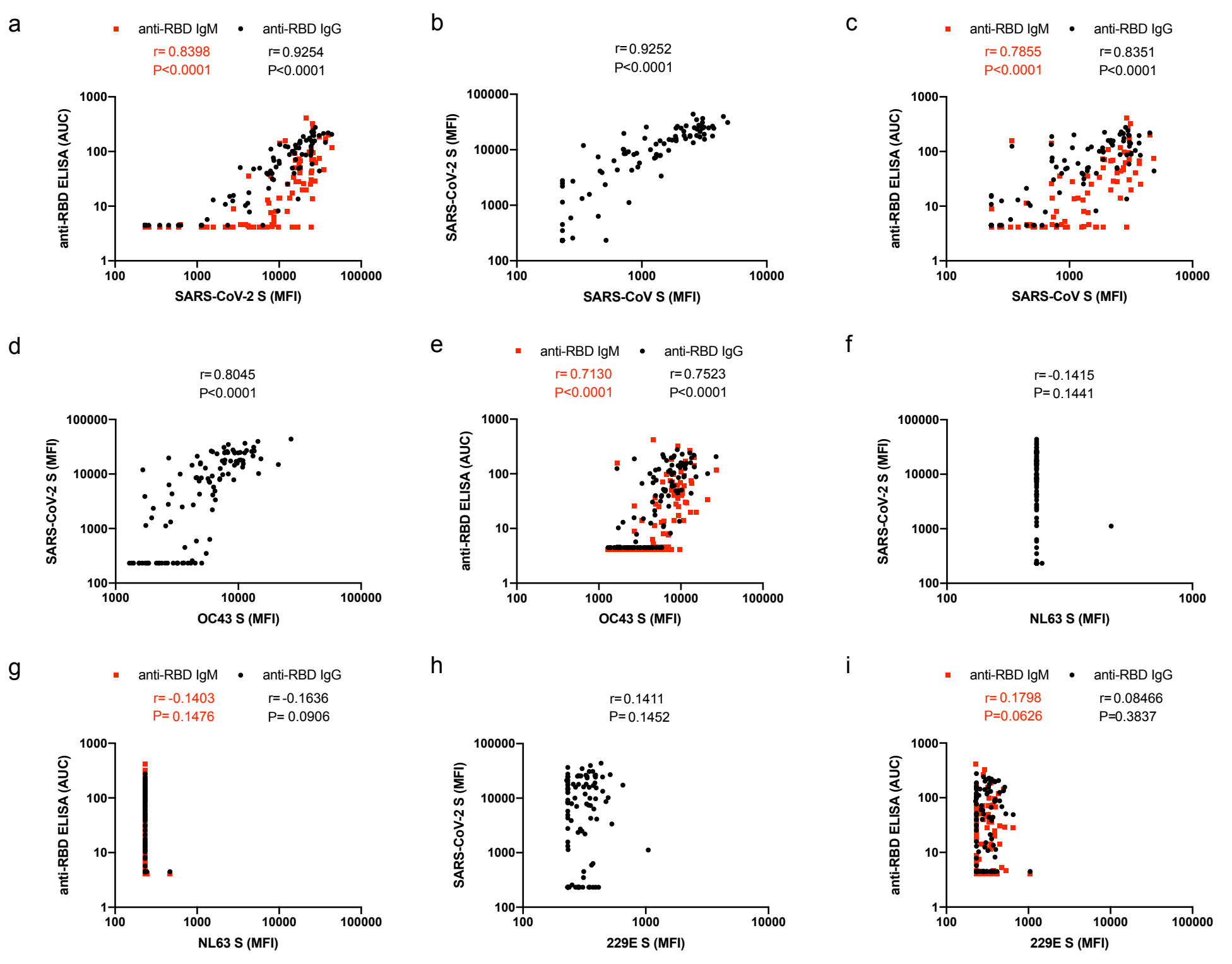
a
anti-RBD IgM
anti-RBD IgG
r= 0.8398
P<0.0001
r= 0.9254
P<0.0001
anti-RBD ELISA (AUC)
SARS-CoV-2 S (MFI)
b
r= 0.9252
P<0.0001
SARS-CoV-2 S (MFI)
SARS-CoV S (MFI)
c
anti-RBD IgM
anti-RBD IgG
r= 0.7855
P<0.0001
r= 0.8351
P<0.0001
anti-RBD ELISA (AUC)
SARS-CoV S (MFI)
d
r= 0.8045
P<0.0001
SARS-CoV-2 S (MFI)
OC43 S (MFI)
e
anti-RBD IgM
anti-RBD IgG
r= 0.7130
P<0.0001
r= 0.7523
P<0.0001
anti-RBD ELISA (AUC)
OC43 S (MFI)
f
r= -0.1415
P= 0.1441
SARS-CoV-2 S (MFI)
NL63 S (MFI)
g
anti-RBD IgM
anti-RBD IgG
r= -0.1403
P= 0.1476
r= -0.1636
P= 0.0906
anti-RBD ELISA (AUC)
NL63 S (MFI)
h
r= 0.1411
P= 0.1452
SARS-CoV-2 S (MFI)
229E S (MFI)
i
anti-RBD IgM
anti-RBD IgG
r= 0.1798
P=0.0626
r= 0.08466
P=0.3837
anti-RBD ELISA (AUC)
229E S (MFI)

293T
293T-ACE2

a

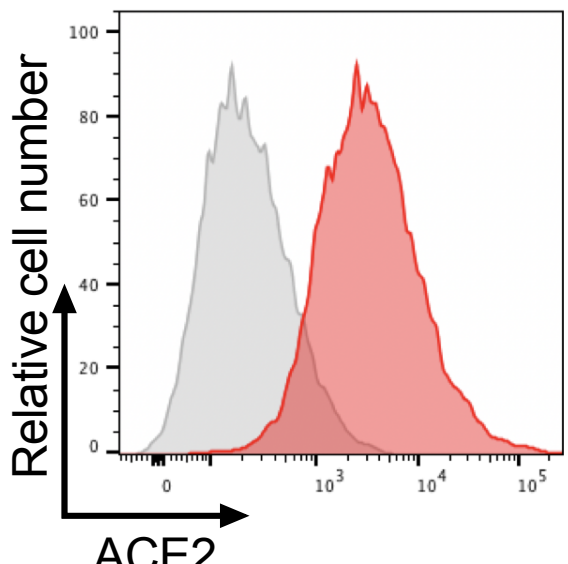

b

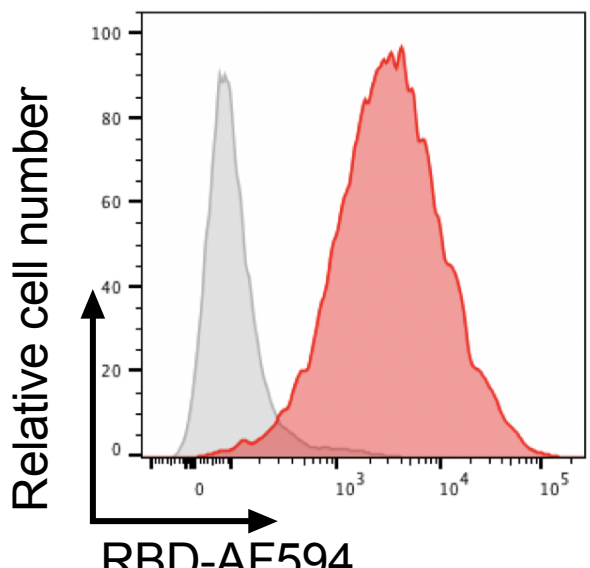

c

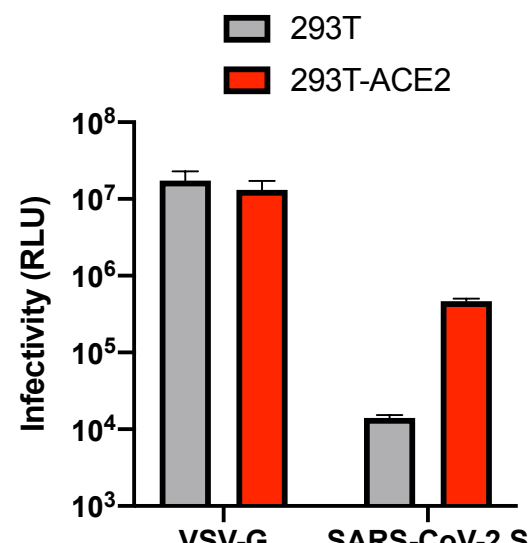

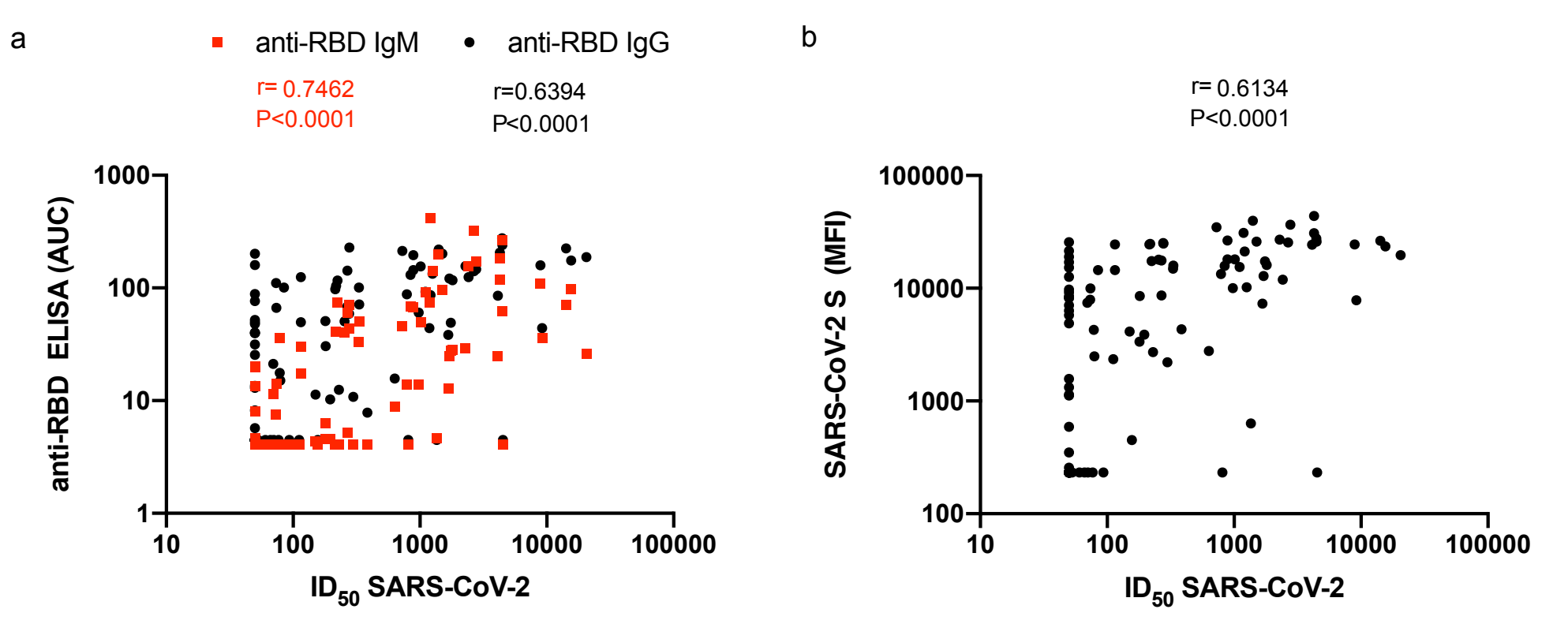
a
anti-RBD IgM
anti-RBD IgG
r= 0.7462
P<0.0001
r=0.6394
P<0.0001
anti-RBD ELISA (AUC)
1000
100
10
1
10
100
1000
10000
100000
ID50 SARS-CoV-2
b
r= 0.6134
P<0.0001
SARS-CoV-2 S (MFI)
100000
10000
1000
100
10
100
1000
10000
100000
ID50 SARS-CoV-2